



Ovarian cancer-derived extracellular vesicles affect normal human fibroblast behavior

Ilaria Giusti, Marianna Di Francesco, Sandra D'Ascenzo, Maria Grazia Palmerini, Guido Macchiarelli, Gaspare Carta & Vincenza Dolo

To cite this article: Ilaria Giusti, Marianna Di Francesco, Sandra D'Ascenzo, Maria Grazia Palmerini, Guido Macchiarelli, Gaspare Carta & Vincenza Dolo (2018) Ovarian cancer-derived extracellular vesicles affect normal human fibroblast behavior, *Cancer Biology & Therapy*, 19:8, 722-734, DOI: [10.1080/15384047.2018.1451286](https://doi.org/10.1080/15384047.2018.1451286)

To link to this article: <https://doi.org/10.1080/15384047.2018.1451286>



Accepted author version posted online: 26 Mar 2018.
Published online: 25 Apr 2018.



Submit your article to this journal [↗](#)



Article views: 78










View Crossmark data [↗](#)

RESEARCH PAPER



Ovarian cancer-derived extracellular vesicles affect normal human fibroblast behavior

Ilaria Giusti [§], Marianna Di Francesco [§], Sandra D'Ascenzo , Maria Grazia Palmerini , Guido Macchiarelli ,
Gaspere Carta , and Vincenza Dolo 

Department of Life, Health and Environmental Sciences, University of L'Aquila, Via Vetoio, Coppito 2, L'Aquila, Italy

ABSTRACT

It has become clear that non-tumor cells in the microenvironment, especially fibroblasts, actively participate in tumor progression. Fibroblasts conditioned by tumor cells become “activated” and, as such, are identified as CAFs (cancer-associated fibroblasts). These CAFs remodel the tumor stroma to make it more favourable for cancer progression. The aim of this work was to verify whether EVs (extracellular vesicles - whose role as mediators of information between tumor and stromal cells is well known) released from human ovarian cancer cells were able to activate fibroblasts. EVs isolated from SKOV3 (more aggressive) and CABA I (less aggressive) cells were administered to fibroblasts. The consequent activation was supported by morphological and molecular changes in treated fibroblasts; XTT assays, zymographies, wound healing tests and invasion assays also highlighted higher proliferation, motility, invasiveness and enzyme expression. The secretome of these “activated” fibroblasts was, in turn, able to modulate the responses (proliferation, motility and invasion) of fibroblasts, and of tumor and endothelial cells. These findings support the idea that ovarian cancer cells can modulate fibroblast behaviour through the release of EVs, activating them to a CAFs-like state; the latter are able, in turn, to stimulate the surrounding cells. EVs from SKOV3 rather than from CABA I seem to be more efficient in some processes.

ARTICLE HISTORY

Received 7 March 2018
Accepted 7 March 2018

KEYWORDS

CAF; Cancer Biology; cancer associated fibroblasts; EVs; endothelial cells; extracellular vesicles; ovarian cancer; tumor microenvironment

Introduction

The term “extracellular vesicles” is used to describe spherical and membrane-enclosed particles that are released by essentially any type of normal or tumor cell into the extracellular space.¹⁻³

EVs have been the subject of intensive studies in the last few years, once it was understood that they were not merely inert cellular debris or artefacts but, instead, bioactive molecular shuttles packaged with proteins, lipids and nucleic acids, that cells use to interact with neighbouring cells to modulate their environment.^{4,5} Moreover, *in vivo*, EVs can travel in almost any biological fluid, exchanging functional information at distant sites and thus representing potential novel biological markers for several pathologies.⁶⁻⁸

As such, EVs are involved in the regulation of many physiological processes, as well as pathological ones;⁹⁻¹⁴ among the latter, cancer represents the most studied process, since EVs contribute to all cancer-related processes, including angiogenesis, invasion, motility promotion and drug resistance.¹⁵⁻¹⁸ EVs are also able to convey messages to stromal cells in order to create a microenvironment supportive of cancer growth, progression and metastasis.¹⁹

The role of the tumor microenvironment has been more strongly appreciated over the last few years, as its ability to

create a loop of intercellular communications that strengthen cancer progression has been highlighted; this is also true for human ovarian cancer, which is one of the leading causes of death due to gynecological malignancy.^{20,21}

The tumor stroma, indeed, accounts for a large percentage of the tumor tissue in ovarian cancer, and is composed of both extracellular matrix components and several cell types, such as endothelial cells, pericytes, immune cells, adipocytes and also fibroblasts, that have been proven to be extremely important in supporting cancer progression.²² Fibroblasts conditioned by tumor cells within the tumor microenvironment acquire specific morphological and molecular features and, as such, these “activated” fibroblasts are identified as cancer-associated fibroblasts (CAFs).²²⁻²⁵ The CAF secretome, in turn, remodels tumor stroma to make it more favorable for tumor progression. In particular, they release tumor-promoting growth factors and chemokines, enhancing the invasive properties of cancer cells, and also molecules that strongly induce angiogenesis and further support the proliferative, migratory and invasive abilities of cancer cells.²³⁻³⁰

Thus, in light of the fundamental role of CAFs in tumor progression, and with consideration of the role of EVs as mediators of information between tumor and stromal cells,

we speculated whether EVs released from ovarian cancer cells were able to activate fibroblasts.

Therefore, the aim of this work was to verify whether extracellular vesicles released from human ovarian cancer cells were able to activate fibroblasts.

Results

Normal fibroblasts treated with EVs acquire CAF morphological features and exhibit their typical markers

Both CABA I and SKOV3 human ovarian cancer cell lines release EVs with intact membrane and various size (Fig. 1). NHDF (normal human dermal fibroblasts) treated with ovarian cancer EVs underwent a morphological change at 72 hours after the beginning of treatment (Fig. 2a); all untreated fibroblasts exhibited the typical elongated and spindle-shaped morphology, while some of the treated fibroblasts were widely spread and showed clearly visible stress-contractile fibers, as the typical morphology of activated fibroblasts.

At the end of treatment with tumor EVs, both untreated and treated fibroblasts were lysed as described and the protein extracts were analyzed to detect the expression of some typical markers of CAFs, such as α -SMA (Fig. 2b) and TIMP-2 (Fig. 2c).

Quantitative analysis detected a significant increase in the expression of α -SMA (calculated molecular weight: ~ 42 kDa) in both NHDF_{CI} (0.5-fold increase, 1.51 ± 0.14 , $p < 0.01$) and NHDF_{SK} (at least 3-fold increase, 3.32 ± 0.10 , $p < 0.01$), when compared with untreated fibroblasts (Fig. 2b). The increase in α -SMA expression induced by the treatment with SKOV3 EVs was statistically significantly higher compared with the increase induced by CABA-I EVs ($p < 0.01$). The expression of TIMP-2 (calculated molecular weight: ~ 24 kDa) was significantly reduced both in NHDF_{CI} and NHDF_{SK} (respectively, 0.68 ± 0.25 , $p < 0.05$ and 0.62 ± 0.16 , $p < 0.05$), while the difference between the two treatments was not statistically significant (Fig. 2c).

Effect of ovarian cancer cell-derived EVs on fibroblast proliferation, motility, invasiveness, enzyme expression and microvesicle release

Proliferation rate was tested at 96, 168 and 264 hours after the start of the EV-administration (Fig. 3a). At shorter durations, CABA I- and SKOV3-derived EVs did not stimulate the fibroblast growth rate, while after 264 h, the proliferation rate significantly increased and decreased, respectively, in NHDF_{SK} and NHDF_{CI}, compared with untreated fibroblasts.

The motility induced by the EV treatment was tested by scratch wound assay (Fig. 3b); migration was repeatedly observed, and the most significant changes were captured at different time intervals (24, 32 and 48 hours) after the starting point (0 hours).

It was clear that, as time went on, more and more cells moved from the wound margins to the center and that, in treated samples, more cells migrated into the wound than in untreated samples (Fig. 3b). To quantify the ability of the cells to close the wound, the wounded area (i.e. the area uncovered from the cells) was measured. The analysis was conducted on images obtained after 32 h and, by convention, the 100% value was assigned to the wound area at time 0; after the considered time interval, the area not yet covered was 57% in untreated fibroblasts (control), whilst it was significantly reduced in EV-treated fibroblasts [40% NHDF_{CI} ($p < 0.01$) and 35% in NHDF_{SK} ($p < 0.01$)] (Fig. 3c).

The invasion assay performed with the modified Boyden chamber showed that fibroblasts treated with EVs had a greater invasive capacity (about 2.5 fold) compared with untreated fibroblasts (Fig. 3d). However, no statistically significant difference was appreciable between the invasive capacities of NHDF_{CI} and NHDF_{SK}.

To estimate whether EV treatment could affect the ability of fibroblasts to secrete proteolytic enzymes, conditioned medium (CM) from EV-treated fibroblasts was normalized according to the same volume and the same cell number, and assayed to evaluate its gelatinolytic and the plasminogen activator activity using zymographies (Fig. 4).

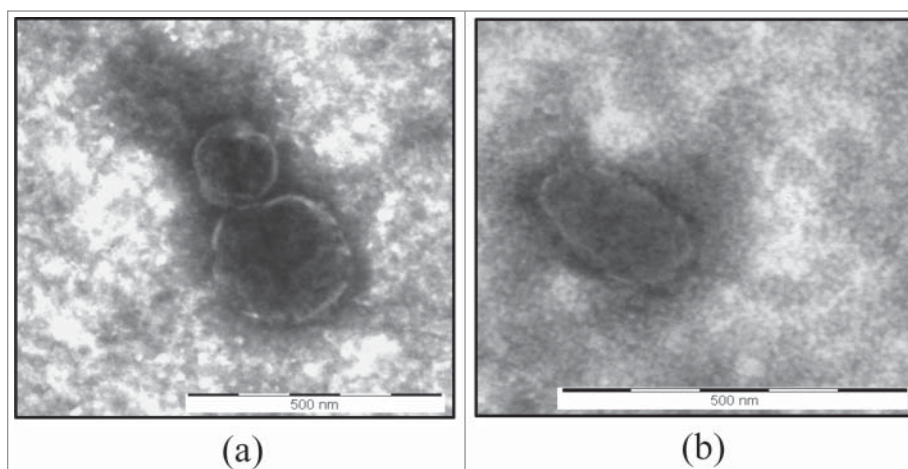


Figure 1. TEM analysis. Transmission electron microscopy images of vesicles isolated from conditioned medium of CABA I (a) and SKOV 3 (b) cells. Displayed vesicles measure 150 nm and 300 nm in Fig. 1a and 300 nm in Fig. 1b. Bar = 500 nm.

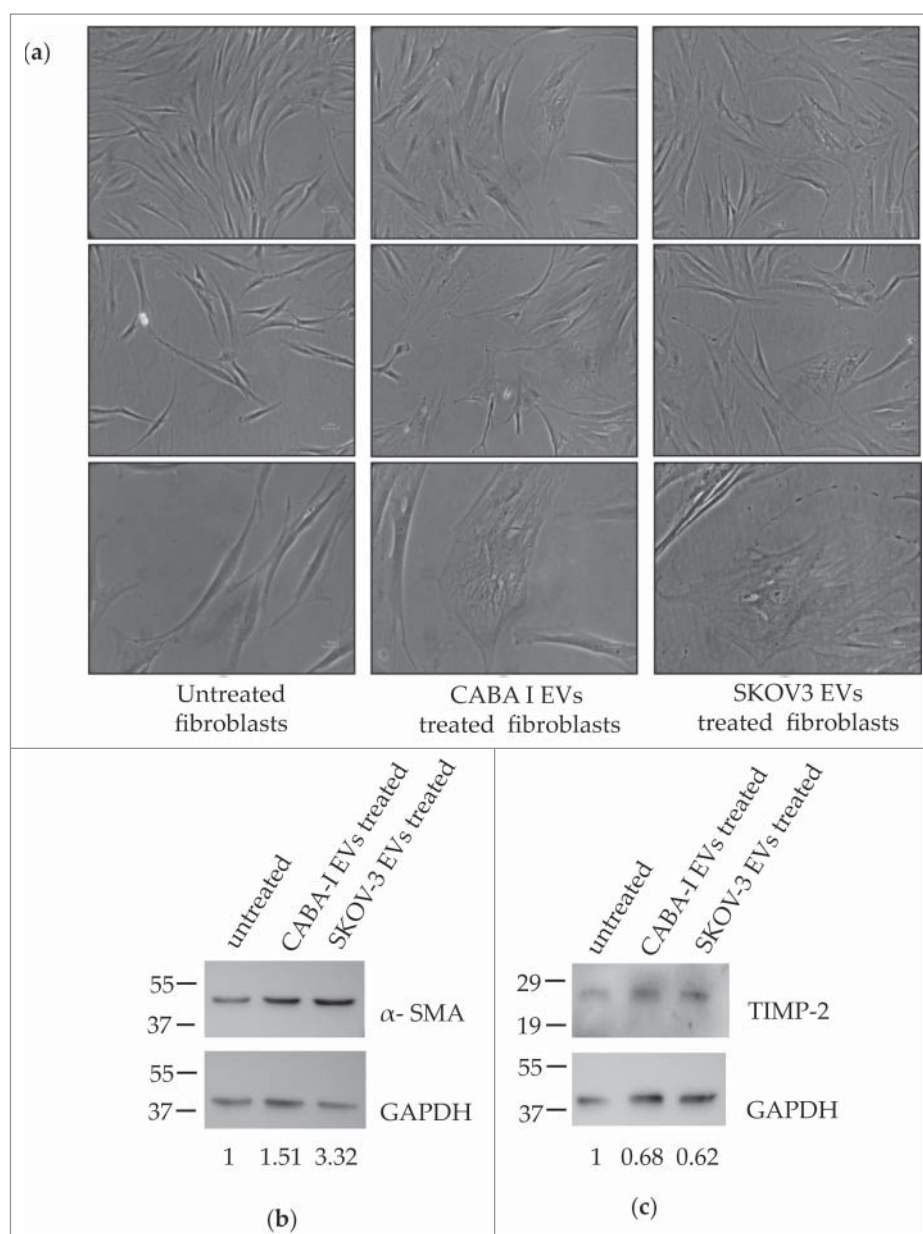


Figure 2. Morphological and markers' expression changes of treated fibroblasts. (a) Representative images of cell morphology: first column from the left shows untreated fibroblasts (NHDF), the second and third ones display NHDF_{Cl} and NHDF_{SK} respectively. The 5X objective of an optical inverted microscope was used to capture images of the first two rows, while pictures of the third row were captured with the 10X objective. The scale bar, which is barely visible, has a size of 1000 nm in all the images. (b-c) Western Blot analysis of α -SMA (b) and TIMP-2 (c); molecular weights (kDa) are reported on the left of each image. Densitometric analysis of the signals were performed with the program Image J and using GAPDH for the normalization. The values of the ratios are shown at the bottom of each panel and the ratio value was conventionally attributed as 1 in untreated fibroblasts.

This assay highlighted the presence in the CM of pro-MMP2 (inactive form of MMP-2), whose secretion was markedly higher in fibroblasts incubated with ovarian cancer cell-derived EVs in comparison to untreated fibroblasts (Fig. 4a); the amount of pro-MMP-2 was almost 2-fold higher (1.71 ± 0.05) in the CM of NHDF_{Cl}, while it was almost 4-fold higher (3.90 ± 0.04) in CM of NHDF_{SK}, and this difference was statistically significant ($p < 0.01$).

Casein-plasminogen zymography also demonstrated the secretion in the CM of high-molecular weight urokinase-type PA (HMW-uPA), the levels of which were increased in fibroblasts after the treatment with EVs (Fig. 4b) The increase was almost 0.5 fold (1.51 ± 0.03) in the CM of NHDF_{Cl}, and it was 2 fold (2.02 ± 0.05) in the CM of NHDF_{SK}. The difference in

HMW-uPA expression between the fibroblasts treated with EVs was determined to be statistically significant ($p < 0,01$).

Fibroblasts (treated and untreated) were also observed to assess whether treatment induced microvesicle (MV) release from the cell surface; the shedding of MVs was very sporadic in control fibroblasts and was limited to small membrane areas, whilst in EV-treated fibroblasts, the extent of the MV release was higher and involved larger membrane areas (Fig. 5).

Secretome of EV-treated fibroblasts affects neighbouring cells

After the end of the treatment with EVs, fibroblasts were grown in DMEM+0.2% LEH for 24 hours, and the

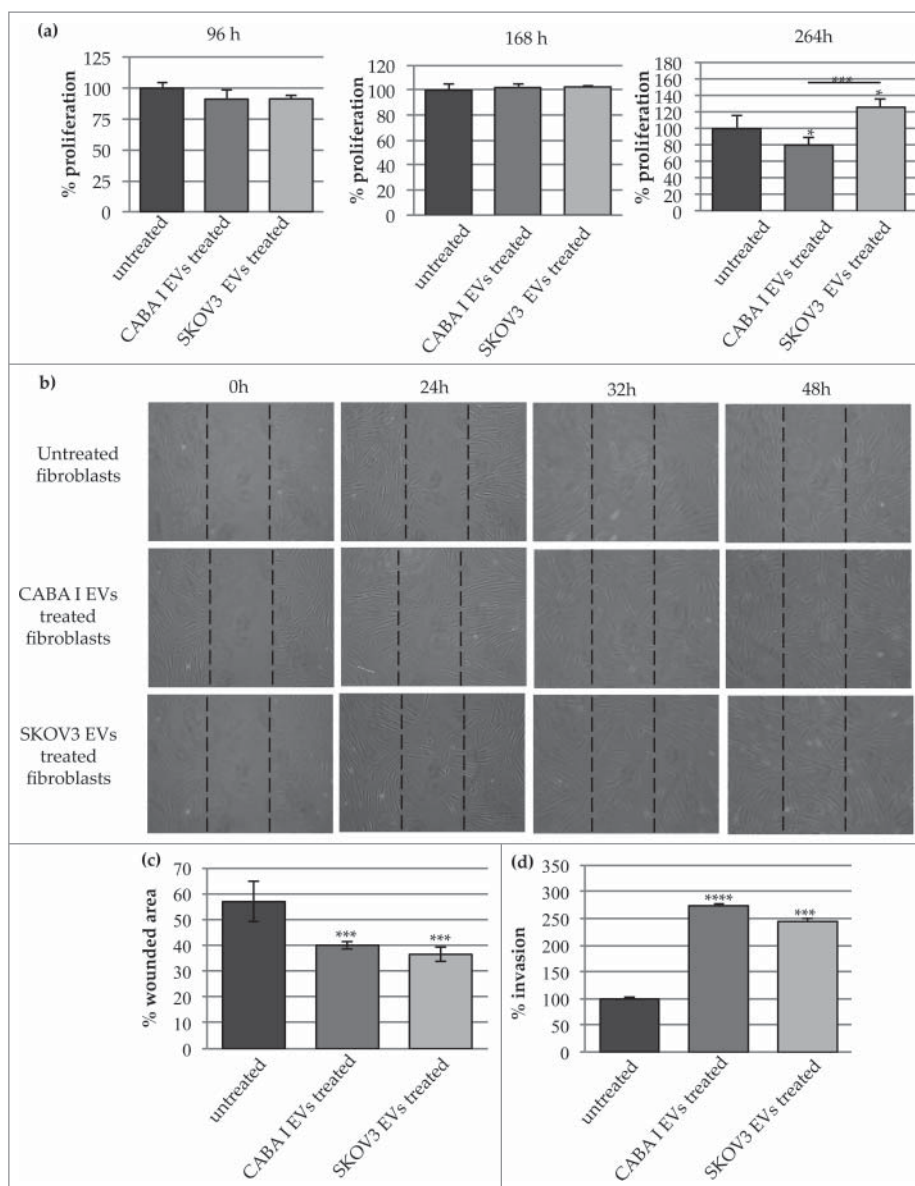


Figure 3. Effects on fibroblasts' proliferation, motility and invasion capabilities. (a) Proliferation test: graphs show proliferation after 96, 168, 264 h; data originated in triplicate and are expressed as mean \pm SD; the value 100% was assigned to untreated fibroblasts. The statistical significance for each sample was calculated compared to untreated fibroblasts (NHDF), while the horizontal line refers to the statistical significance between NHDF_{CI} and NHDF_{SK} ($*p < 0,05$; $**p < 0,01$). (b) The effects of CABA I and SKOV3 derived EVs on fibroblasts' migration determined by wound-healing assay: a summary panel showing fibroblasts' migration in untreated and EVs-treated fibroblasts (rows) after 24, 32 and 48 hours (columns). Images at 0 h represent the initial wound area; dotted lines define the size of the original scratch. (c) Graph shows the % of wounded area 32 hours after the beginning of the assay; the original scratch area was conventionally assumed as 100%. The area of the scratch was measured through the software Image J and values were shown as mean \pm SD of three independent experiments. (d) The number of invaded fibroblasts through the Matrigel coated filter was counted in 5 random fields per each well of the modified Boyden chamber with the objective 20X of an inverted optical microscope. Data are reported as mean \pm SD; the statistical analysis was referred to untreated fibroblasts (NHDF), whose invasion was conventionally set as 100%. ($**p < 0,01$).

conditioned media (CM) containing molecules secreted by untreated and EV-treated fibroblasts were used as stimuli to evaluate their effect on cells normally present in the tumor microenvironment, such as fibroblasts, endothelial cells and tumor cells.

Fibroblast proliferation assays showed that the CM from untreated and EV-treated fibroblasts did not increase the growth rate of normal fibroblasts (Fig. 6a) but, instead, promoted significant migration of normal fibroblasts (Fig. 6b); migration of fibroblasts toward the medium conditioned by EV-treated fibroblasts was about 50% increased with respect to their migration toward the medium conditioned by untreated

fibroblasts, although no differences were appreciable between medium conditioned by NHDF_{CI} or NHDF_{SK}.

To analyze the effects induced by fibroblasts exposed to ovarian cancer cell-derived EVs on the same ovarian cancer cells, their migratory and invasive abilities were tested, in addition to their proliferative capacity, in response to the CM.

The proliferative ability of CABA I and SKOV3 cells was not affected by CM (Fig. 7a and 7b, respectively). On the contrary, the migratory abilities of ovarian cancer cells were significantly promoted; they were higher in response to the CM of fibroblasts treated with EVs than in response to the CM of untreated fibroblasts. In particular, while CABA I cells migrated at a

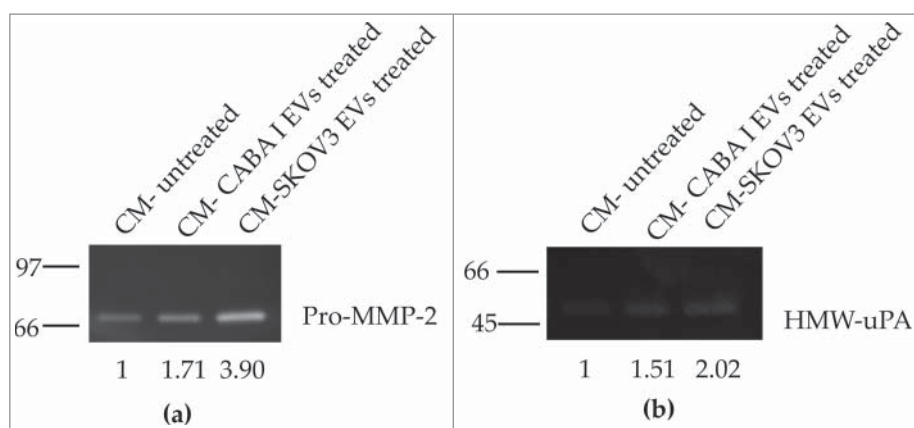


Figure 4. Zymography assays. (a) Gelatin zymography was performed for MMP-2 and MMP-9 detection. (b) casein-plasminogen zymography was performed for Plasminogen Activators (PAs) detection. Levels of pro-MMP-2 (~72 kDa) and HMW-uPA (~50 kDa) were quantified by densitometric analysis in all samples. Values are reported on the bottom of figures, and are in proportion to the band of untreated fibroblast (NHDF) that was set conventionally at 1.

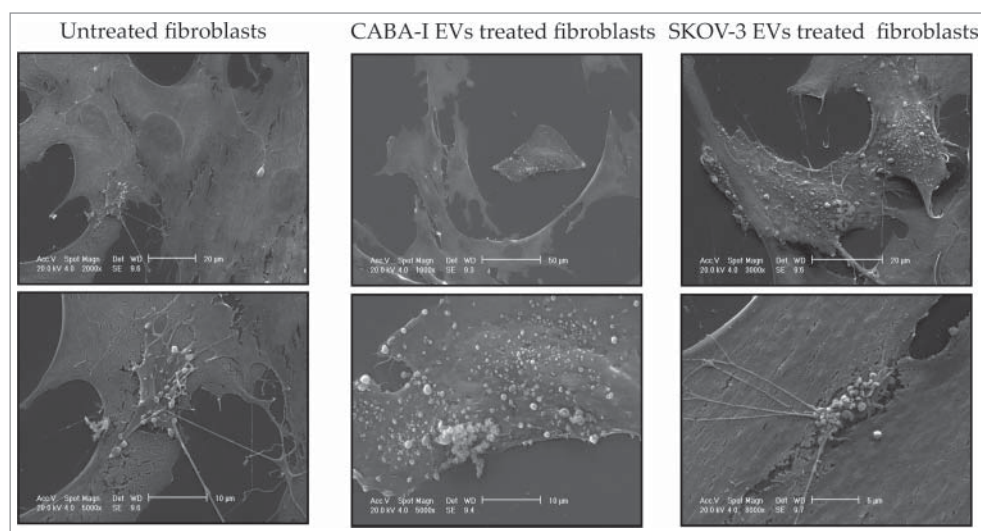


Figure 5. Scanning Electron Microscopy (SEM). The first upper row is composed of low-magnification images, the second one shows some details of the cell surface at higher magnification, clearly exhibiting the phenomenon of the shedding of microvesicles. Reported images are representative of the experiments that evidenced in NHDF_{Cl} and NHDF_{SK} an abundant microvesicles release on the cell surface, while in untreated fibroblasts (NHDF) shedding of microvesicles was extremely sporadic.

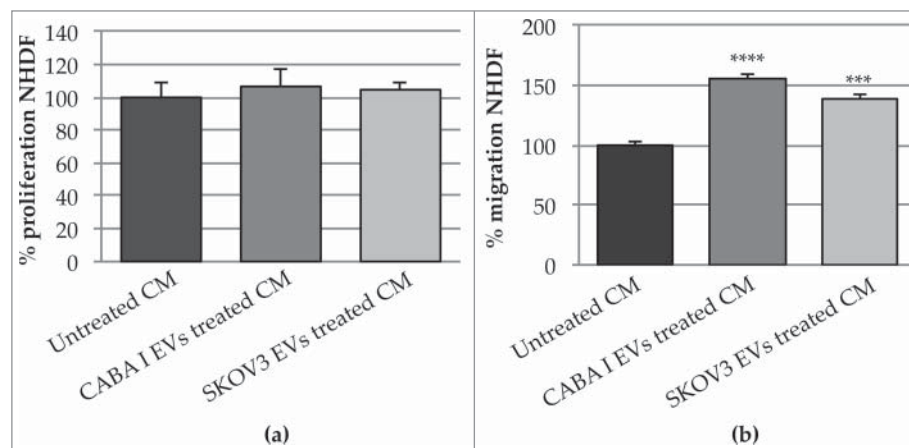


Figure 6. Effects of the CM from untreated and treated fibroblasts on neighbouring fibroblasts (a): proliferation of fibroblast treated with CM NHDF, CM NHDF_{Cl} and CM NHDF_{SK}. Data (means±SD) were represented as percentage and the proliferation of fibroblasts treated with CM NHDF was set 100%. (b): fibroblasts migration assay in presence of CM from untreated and EVs treated fibroblasts. Data (means±SEM) were represented as percentage and the migration of fibroblasts treated with CM-untreated was set 100%. (** $p < 0,01$).

similar rate toward both types of CM (from NHDF_{CI} or NHDF_{SK}) (Fig. 7c), SKOV3 cells seemed to migrate preferentially in response to the CM of NHDF_{SK} over the CM of NHDF_{CI} (Fig. 7d).

CM from fibroblasts exposed to EVs induced further modulation in cancer cells, by affecting their invasive behaviour. Ovarian cancer cells, exposed *in vitro* to the CM of fibroblasts treated with EVs, showed an enhanced invasive capacity, of which the trend was the opposite of the one observed for motility. CABA I cell invasion was more stimulated by the CM of NHDF_{SK} than by the CM of NHDF_{CI} (Fig. 7e), while SKOV3 cells migrated similarly toward both types of CM (Fig. 7f).

HUVECs were stimulated with CM to assess their motility response. HUVEC migration was identified via scratch

wound healing assay, and the most marked changes were captured at different time intervals (7, 9 and 24 hours) after the beginning point (0 hours) (Fig. 8a). CM from NHDF_{CI} more efficiently stimulated wound closure, as confirmed by quantification of the scratch area at 24 hours; the scratch area decreased to 71% (where 100% was assigned to the original scratch area) in HUVECs treated with the CM of untreated fibroblasts and, significantly, to 53% in HUVECs treated with the CM of NHDF_{CI} ($p < 0.01$), while no significant decrease in the scratch area was identified in HUVECs exposed to the CM of NHDF_{SK} in which the percentage of the still wounded area was 79% (Fig. 8b).

In addition to HUVEC migratory capacity, we also tested whether CM from fibroblasts treated with ovarian cancer cell-

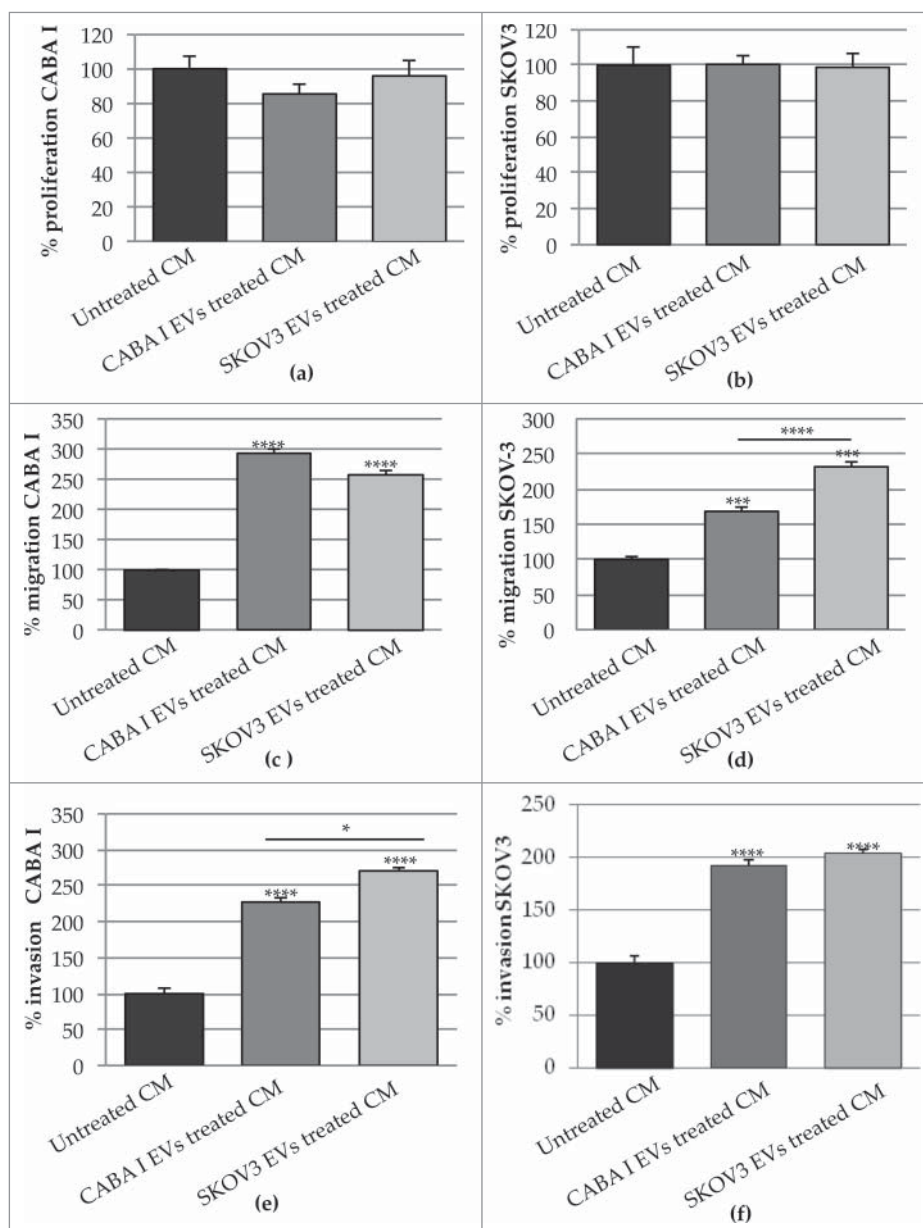


Figure 7. Effects of the CM from untreated and treated fibroblasts on neighbouring cancer cells. (a-b) The proliferation of CABA I (a) and SKOV3 (b) was tested in presence of the CM NHDF, CM NHDF_{CI} and CM NHDF_{SK}. Data are shown as mean \pm SD and were representative of three independent experiments. 100% proliferation was assigned to ovarian cancer cells treated with CM NHDF. (c-d) Migration ability of ovarian cancer cells, CABA I (c) and SKOV3 (d) cells, following exposure to CM NHDF, CM NHDF_{CI} and CM NHDF_{SK}, through a modified Boyden chamber. Data are expressed as mean \pm SEM and the value 100% migration was assigned to cells migrating in response to the CM NHDF. (e-f) The *in vitro* cell invasion assay, performed with the modified Boyden chamber, of CABA I (e) and SKOV3 (f) cells. Data, expressed as mean \pm SEM, were shown as percentage of invading cells and 100% invasion was attributed to fibroblasts invading towards CM NHDF (* $p < 0,05$; ** $p < 0,01$).

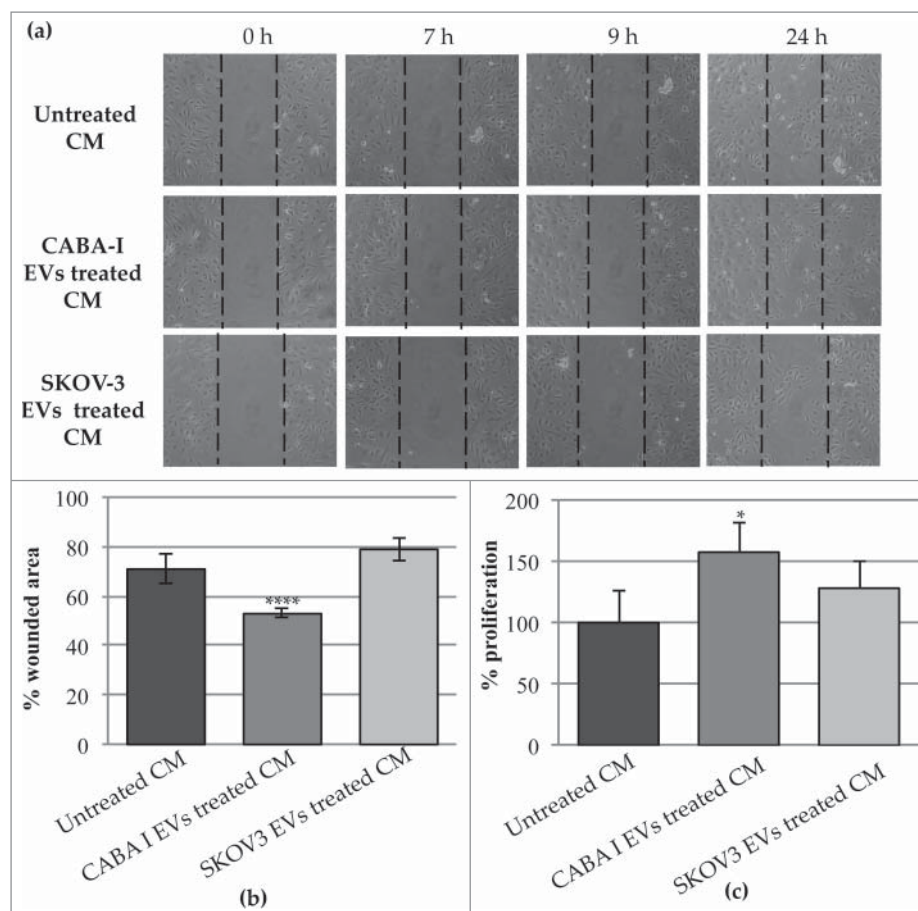


Figure 8. Effects of the CM NHDF, CM NHDF_{Cl} and CM NHDF_{SK} on motility and proliferation of neighbouring HUVEC cells. (a): The scratch area was monitored at multiple times over a 24 hours-period. Images of the most significant time intervals (beginning point = 0 hour, 7 hours later, 9 hours later and 24 hours) were captured. Dotted lines represent the size of original scratch. (b): Graph showing the % of wound area of the scratch at 24 hours after the creation of the scratch (0 h) (original wounded area was set, for each condition, as 100%). The percentages of the scratch area were calculated as mean±SD of three independent experiments (***p* < 0,01). (c): The proliferation was measured and expressed as percentage of proliferating HUVECs. The value 100% proliferation was assigned to CM NHDF-treated HUVEC (**p* < 0,05).

derived EVs could promote proliferation. Stimulation by the CM from EV-treated fibroblasts induced proliferation in HUVEC cells, but only with the CM of NHDF_{Cl} was the increase statistically significant (Fig. 8c).

Discussion

Some studies have already reported the role of EVs in the activation of tumor stromal cells,³¹⁻³⁶ while little is known of the mechanisms used by ovarian cancer cells to transform normal fibroblasts into CAFs.³⁷ To the best of our knowledge, none of the aforementioned works considered human ovarian cancer-derived EVs and their eventual contribution to the activation of normal fibroblasts. CAFs, indeed, can originate via several mechanisms: they may be derived from epithelial or endothelial cells, from pericytes, adipocytes and circulating mesenchymal stem cells.³⁸⁻⁴⁰ CAFs, however, can also originate from the activation of resident fibroblasts mediated by growth factors released from tumor cells.^{23,38-40}

The aim of the present study was to characterize the contribution of ovarian cancer cell-derived EVs in inducing the transition of normal fibroblasts into CAFs.

For this purpose, we isolated EVs from two human ovarian cell lines, CABA I and SKOV3, characterized by differing aggressiveness in terms of invasive capabilities and

proangiogenic capacities (lower in CABA I and higher in SKOV3),^{15,41} and evaluated their effect on normal human dermal fibroblasts (NHDF), cells already used as model of stromal fibroblasts in other studies.^{42,43}

EVs isolation was carried out by mean of differential centrifugation/ultracentrifugation that is one of the most used methods for EVs isolation;⁴⁴ by Transmission Electron Microscopy we also verified the structural integrity and purity of EVs samples.

Along with many other molecules, TGF- β is the main factor responsible for the recruitment of activated fibroblasts in many types of cancer;^{38,40} in light of this, preliminarily, the presence of TGF- β was verified in CABA I and SKOV3 EVs through western blotting, and was demonstrated to be associated with both of them, with a higher level in SKOV3 EVs (data not shown).

To reproduce, *in vitro*, the continuous stimulation of fibroblasts by cancer cell EVs that we suppose takes place *in vivo*, the NHDF were administered with 1 μ g CABA I or SKOV3-derived EVs/ml daily for up to 5 days, in a cumulative way (adding the new dose of EVs to the previous one without replacing the medium throughout the treatment).

Upon exposure to ovarian cancer cell EVs, amidst normal fibroblasts, easily recognizable for their typical elongated and spindle-like shape, some cells exhibited a very

large shape characterized by visible contractile stress fibers, which is the typical morphology of activated fibroblasts; indeed, CAFs typically display a “spread” phenotype similar to that of myofibroblasts involved in wound healing processes.^{23,25} The identity of treated cells as activated fibroblasts was confirmed by marker analysis; common markers for CAFs include α -SMA, along with SDF-1, FSP-1, vimentin, desmin, tenascin and FAP α .^{22,24,25,38} We identified α -SMA expression to be increased compared with untreated fibroblasts. The expression of TIMP-2 was also assessed (it was demonstrated that the loss of the TIMP gene family is sufficient for the acquisition of the CAF-like cellular state);⁴⁵ its expression decreased both in NHDF_{CI} and NHDF_{SK}. For the expression of both molecules, NHDF_{SK} showed the most pronounced change.

Such morphological and molecular changes supported the idea that ovarian cancer-derived EVs can induce an activation-like state in fibroblasts.

Since CAFs have enhanced proliferative, migratory and invasive abilities²³ we tested whether EV-activated fibroblasts shared these features, and confirmed the ability of EVs to induce NHDF proliferation, motility and invasiveness. No differences in proliferation rate were evident shortly after EV treatment (96 and 168 hours), while after 264 hours, the growth rate of fibroblasts treated with EVs from SKOV3 was higher than both untreated cells and NHDF_{CI}. On the contrary, no statistically relevant differences were evident between the NHDF_{CI} and NHDF_{SK} with respect to migratory and invasive capacities, even if both these processes were statistically significantly stimulated in treated fibroblasts; they were probably sustained by the increased amount of proteolytic enzymes (gelatinases and PAs) released from treated fibroblasts compared with untreated ones. It is already known, in fact, that CAFs produce MMPs that, in degrading the extracellular matrix, facilitate cancer cell migration and invasion.^{23,24,26}

Ovarian cancer EV-treated fibroblasts also displayed an increased release of MVs from the cell surface, confirming their activated state; it was already demonstrated that the extensive production of MVs by CAFs is used as a means to move lipids and proteins to target cancer cells in order to support tumor growth.⁴⁷ The release of MVs from the cell surface of treated fibroblasts more closely resembled what is observed in tumors than in normal cells: MVs were released in higher numbers than in untreated fibroblasts, and the release was not restricted to specific membrane areas (as is usually the case in normal cells³ and, indeed, was visible in untreated cells), but involved large areas (NHDF_{SK}) if not the whole surface (NHDF_{CI} and NHDF_{SK}).

Some studies have already suggested that fibroblasts and, particularly, CAFs can actively modulate neighbouring cells in the tumor microenvironment; crosstalk between ovarian cancer cells and CAFs is known to promote the motility and invasion of cancer cells and is mediated, at least partly, by TGF- β .²² This crosstalk could rely also on the release of exosomes: fibroblast-derived exosomes, for example, stimulate motility in breast cancer cells,⁴⁸ while CAF-derived exosomes can lead to increased drug resistance by modulating the percentage clonogenicity and tumor growth of cancer

stem cells in colorectal cancer.⁴⁹ Therefore, based on the knowledge of the role of CAFs in modulating the surrounding cells, knowing that fibroblasts activated by tumor-derived EVs induced an increased release of MVs, and being aware of the role of EVs in the crosstalk between cells, we evaluated whether our activated fibroblasts were actually able to modulate the response of some cells usually present in the tumor microenvironment, such as fibroblasts themselves, and tumor and endothelial cells.

For purely technical reasons, due to a material shortage, we did not use the EVs isolated from the fibroblasts, but instead their conditioned medium (which, however, contains the EVs too).

These conditioned media contain all soluble and EV-associated molecules released by untreated and EV-treated fibroblasts, and were used to evaluate their effect on cells normally present in the tumor microenvironment, such as normal/stromal fibroblasts (autocrine effects), ovarian cancer cells and endothelial cells (paracrine effects). The secretome of fibroblasts and CAFs has been already proven, *in vitro*, to be involved in tumor-microenvironment crosstalk in several cancers,^{50,51} but no studies, to the best of our knowledge, have assessed its effects in human ovarian cancer.

The conditioned medium from fibroblasts treated with EVs did not significantly affect the proliferation of normal stromal cells, such as fibroblasts, nor of tumor cells, with the latter disagreeing with some studies reported in literature on different types of cancer cells,^{52,53} but did slightly increase the proliferation of endothelial cells; on the other hand, the conditioned medium significantly affected the motility and invasiveness of all these cells.

Curiously, even though EVs isolated from both ovarian cancer cell lines were able to activate fibroblasts, EVs released from the more aggressive cells (SKOV3) seemed to be more efficient in some processes (higher marker expression, proliferation, enzyme release) than the less aggressive cells (CABAI). Similarly, even though the conditioned media from NHDF_{CI} and NHDF_{SK} was able to stimulate cancer cell motility and invasiveness, SKOV3 motility and CABA I invasiveness were more induced by NHDF_{SK} conditioned medium. With endothelial cells, the opposite effect was observed: NHDF_{CI} conditioned medium was more efficient at motility and proliferation induction. These data, overall, led us to hypothesize that EVs with different messages derive from different cells; but, also, that the specific response to different stimuli strongly depends on the identity of the target cells.

Our findings support the idea that ovarian cancer cells can modulate fibroblast behaviour, through the release of EVs that induce phenotypic and functional changes in normal stromal fibroblasts, activating them to a CAF-like state; these CAF-like cells are able, in turn, to stimulate some abilities in the surrounding normal and tumoral cells. EVs released from a more aggressive cell line (SKOV3), moreover, seem to be more efficient in the stimulation of some processes compared with EVs released from a less aggressive cell line (CABA I). EV-associated TGF- β could be one of the molecules responsible for these processes.

Materials and methods

Cell cultures

The CABA I is an ovarian carcinoma cell line,⁵⁴ while SKOV3 cells derived from malignant ascites of ovarian adenocarcinoma patients and were purchased from the ATCC (American Type Culture Collection). Cells were grown as monolayers in RPMI-1640 containing, respectively for CABA I and SKOV3 cells, 5% (v/v) and 10% (v/v) heat-inactivated FBS (fetal bovine serum), supplemented with 1X penicillin/streptomycin and 2 mM L-glutamine.

The human normal fibroblast cell line NHDF (normal human dermal fibroblasts), obtained from adult skin, were purchased from Lonza Group, Ltd. (Basel, Switzerland) and grown in DMEM + 10% FBS, 2 mM glutamine, penicillin and streptomycin. Cells were subcultured and used within the 15th passage, as suggested by Lonza's protocols.

HUVECs (human umbilical vein endothelial cells) were purchased from Lonza Group, Ltd. and were grown at 37°C with 5% CO₂ in 1% gelatin-coated flasks, in DMEM supplemented with 10% FBS, 10% NCS (newborn calf serum), 20 mM HEPES [N-(2-hydroxyethyl)piperazine-N'-(2-ethanesulfonic acid)], 6 U/mL heparin, 2 mM glutamine, 50 µg/mL ECGF (endothelial cell growth factor), penicillin and streptomycin. The cells were used between the third and fifth passage.

All cell lines were cultured at 37°C in a humidified atmosphere with 5% CO₂. All the experiments were carried out when the cells were sub-confluent and mycoplasma-negative.

FBS, RPMI, DMEM, glutamine, penicillin and streptomycin were purchased from Euroclone (Euroclone SpA); Hepes and ECGF from Sigma-Aldrich (Merck KGaA); and NCS from Gibco (Thermo Fisher Scientific).

EV isolation from culture media

To isolate EVs, CABA I and SKOV3 cells were grown in 5% 40 nm-filtered FBS HyClone (GE Healthcare) in RPMI-1640; the medium was centrifuged at 600 × g for 15 minutes, and then at 1500 × g for 30 minutes to remove cells and large debris, respectively. The supernatants were centrifuged at 100000 × g for 2 hours at 4°C in a Beckman ultracentrifuge. Pelleted EVs were resuspended in Dulbecco's phosphate-buffered saline (EuroClone). Two repeat EV quantifications were carried out by measuring the EV-associated protein amounts using the Bradford method (Bio-Rad) with BSA (bovin serum albumin; Sigma-Aldrich; Merck KGaA) as the standard.

Electron microscopy

Transmission electron microscopy (TEM) was performed on isolated vesicles, resuspended in PBS, to analyze their ultra-structural morphology. According to proper dilutions, the samples were adsorbed to 300 mesh carbon-coated copper grids (Electron Microscopy Sciences, Hatfield, PA, USA) for 5 minutes in a humidified chamber at room temperature. Vesicles on grids were then fixed in 2% glutaraldehyde (Electron Microscopy Sciences, Hatfield, PA, USA) in PBS for 10 minutes and then briefly rinsed in milli-Q water. Grids with adhered vesicles were examined with a Philips CM 100

transmission electron microscope TEM at 80 kV, after negative staining with 2% phosphotungstic acid, brought to pH 7.0 with NaOH. Images were captured by a Kodak digital camera.

Scanning electron microscopy (SEM) analysis was performed on fibroblasts that were treated with EVs for up to 5 days. 48 hours after the end of this treatment, untreated and EV-treated fibroblasts were detached and allowed to grow to subconfluence on coverslips for an additional 96 hours, then samples were prepared for SEM analysis by fixing in 2% glutaraldehyde (Electron Microscopy Sciences, Hatfield, PA, USA) in phosphate-buffered saline (PBS) for 3 minutes.

After being critically dehydrated with a graded scale of ethanol (30% to 100%) and point-dried, the samples were glued onto stubs, coated with gold in a SCD040 Balzer Sputterer, and detected with a Philips 505 SEM at 20 kV.

Fibroblast treatments with ovarian cancer cell derived-EVs

NHDFs were treated with EVs from CABA I or SKOV3 cells, supplying 1 µg EVs/ml every day up to 5 days in a cumulative manner. EVs were added every 24 hours without replacing the medium for the entire duration of the treatment with EVs, in order to mimic the continuous release of EVs from cancer cells within the tumor microenvironment and the persistent exposure of fibroblasts to EVs.

Treatments were performed by adding EVs to the culture media supplemented with a reduced percentage of FBS (2%), in order to decrease the stimulatory effect of the serum while ensuring fibroblast survival.

NHDFs treated with EVs from CABA I or SKOV3 cells are respectively indicated as NHDF_{CI} and NHDF_{SK} throughout the text.

Collection of fibroblast conditioned medium (CM)

To verify whether treated NHDFs modify their secretome, after the 5-day cumulative treatment with 1 µg EVs/ml, cells were washed with serum-free DMEM and then incubated for 24 h in complete medium in which the FBS was replaced with 0.2% LEH (lactalbumin enzymatic hydrolysate; Sigma-Aldrich; Merck KGaA), to remove the effect of enzymes/growth factors from the serum. In parallel, CM was prepared from untreated fibroblasts (controls) in the same manner. In all the collected CM, cells and cell debris were discarded. Then, CM was used for cellular tests such as proliferation, migration and invasion assays, in addition to gelatin zymography assays, or was concentrated using Centricon Ultracel YM-10 filters (Amicon Bio-separations; Millipore Corporations; cutoff, 10 kDa) to be analyzed via casein-plasminogen zymography assays.

Western blots

48 hours after the end of the 5-day treatment with EVs, NHDF_{CI} or NHDF_{SK} were washed three times with PBS and lysed in RIPA Lysis Buffer, containing 50 mM Tris-HCl, pH 7.5; 150 mM NaCl; 0.5% sodium deoxycholate; 1% Triton-X; 0.1% sodium dodecyl sulfate (SDS); 5 mM EDTA; 100 mM sodium fluoride (NaF); 2 mM sodium orthovanadate (Na₃VO₄); 10 mM sodium pyrophosphate (NaPPi); 1 mM phenylmethylsulfonyl fluoride

(PMSF); and a classical protease-inhibitor cocktail (Sigma-Aldrich; Merck KGaA). The protein content was determined via Bradford protein assays. Samples containing 15 μg protein were resolved by SDS-PAGE on a 12.5% gel to identify the expression of α -SMA (α -smooth muscle actin) under reducing conditions and with heating, and of TIMP-2 (tissue inhibitor of metalloproteinase-2) under non-reducing conditions and without heating.

Separated proteins were then blotted on nitrocellulose membrane (Whatman-GE Healthcare Life Sciences). Non-specific binding sites were blocked for 2 hours in 10% non-fat dried milk in TBS containing 0.5% Tween-20 (TBS-T) at room temperature.

Subsequently, the blots were probed with specific primary Abs at 4°C overnight: α -SMA (rabbit monoclonal, 1:5000 dilution, cat. no. ab32575-100, Abcam) and TIMP-2 (mouse monoclonal, 1:200 dilution, cat. no. MA5-13603, Thermo Fisher Scientific, Inc.). GAPDH (mouse monoclonal, 1:500 dilution; cat. no. MA5-11114; Thermo Fisher Scientific, Inc.) staining was used for normalization.

After several washes in TBS-T, the membranes were incubated in corresponding horseradish peroxidase (HRP)-conjugated secondary Abs: goat anti-mouse IgG-HRP, dilution 1:10000 and goat anti-rabbit IgG-HRP, dilution 1:7500 (both Santa Cruz Biotechnolog, Inc.) for 1 h.

All the antibodies were diluted in blocking buffer (TBS-T containing 1% non-fat dry milk).

After washing in TBS-T, the reactive bands were visualized with a chemiluminescence detection kit (Super Signal West Femto Chemiluminescent Substrate, Thermo Fisher Scientific, Inc. for all bands, except for GAPDH, which was visualized with SuperSignal West Pico Chemiluminescent Substrate, Thermo Fisher Scientific, Inc.).

Images were recorded and analyzed with the gel documentation system Alliance LD2 (Uvitec).

Proliferation assays

NHDF (1000 cells/well) were seeded onto a 96-well plate and incubated for 24 h in complete medium at 37°C and 5% CO₂, to facilitate cell adhesion and spreading. Then, fibroblasts were treated, as specified above, with CABA I or SKOV3 EVs, 1 $\mu\text{g}/\text{ml}/\text{day}$ for 5 days. The effects on proliferation were evaluated by XTT assay at 96, 168 and 264 hours after the beginning of the EV treatment. Untreated fibroblasts, grown in the same medium but without EVs, were used as the control.

For experiments with conditioned medium (CM), NHDF (1000 cells/well), HUVECs (1000 cells/well) and the CABA I and SKOV3 ovarian cancer cells (1500 cells/well) were seeded into 96-well plates (gelatin-coated for HUVECs), and allowed to adhere and spread for 24 hours at 37°C and 5% CO₂, then cultured for 96 hours (NHDF) or 72 hours (HUVECs, CABA I, SKOV3) with the CM obtained from NHDF_{CI} or NHDF_{SK}; at the end of each specified interval, the proliferation was assessed via XTT assay. During the experiments on NHDFs, CM was supplemented with 1% FBS, in order to ensure fibroblast survival without stimulating their growth, whereas the CM for the HUVEC experiments was supplemented with 5% FBS, 5% NCS, HEPES, Eparin and ECGF, in order to guarantee HUVEC survival without encouraging their growth; CABA I and

SKOV3 cells were incubated with non-supplemented CM. Cells incubated with CM from untreated fibroblasts were used as controls.

For the XTT (2,3-Bis (2-methoxy-4-nitro-5-sulphophenyl)-2H-tetrazolium-5-carboxanilide) assay, 1 mg/ml XTT (Sigma-Aldrich; Merck KGaA) and 1,53 mg/ml phenazine methosulfate (PMS, Sigma-Aldrich; Merck KGaA) were mixed, and 50 μL of this solution was added to each well. Plates were incubated for 4 hours at 37°C with 5% CO₂; after this interval, the optical density (OD) was measured using an ELISA (enzyme-linked immunosorbent assay) reader at 450 nm. XTT tests were performed before the cells reached confluence to prevent possible artifact decreases in the results due to contact inhibition.

Each experiment was performed in triplicate and repeated at least twice. The data are expressed as the means \pm standard deviations (SD).

In vitro scratch wound healing assay

The wound healing assay is one of the earliest developed tests to study directional cell migration *in vitro*, and is based on the observation of cell migration into a scratch “wound” created on a cell monolayer; this assay was used to study both HUVEC and NHDF migration.

Cells were cultured in 24-well microplates under normal culture conditions and allowed to reach confluence. A previously-sterilized 200 μl plastic tip was drawn across the cellular stratum to produce a wound, floating cells were removed, and wells were washed 3 times with PBS to remove debris and smooth the edge of the wound.

For NHDFs, the scratch was performed at 48 hours after the end of the 5-day treatment with EVs, and cells were subsequently grown in FBS-reduced culture medium (2% FBS), avoiding scratch closure due to cell growth. The scratch was monitored for 48 hours.

HUVECs were cultured in the CM of untreated and EV-treated fibroblasts, supplemented with 1% FBS (in order to guarantee cell survival but, in the meantime, avoiding the closure of the wound due to cell proliferation) Hepes, Eparin and ECGF, for 24 hours.

The status of the scratch wounds was monitored using a phase-contrast microscope at the beginning of the assay and at regular intervals, and representative images were collected.

Invasion assays

For the study of cell invasiveness, modified Boyden chambers were used, dividing the upper and the lower compartments with filters (8- μm pore size polycarbonate polyvinylpyrrolidone-free Nucleopore filters) coated with a thin layer of Matrigel® Growth Factor-reduced (BD Biosciences) and diluted in serum-free medium to a concentration of 0.5 mg/ml.

Briefly, untreated and EV-treated fibroblasts (1000 cells/well) were added to the upper chamber in 45 μL serum-free medium, and medium containing 10% FBS was added into the lower chamber as a chemoattractant; untreated invading fibroblasts were used as controls.

In the experiments with ovarian cancer cells, CABA I or SKOV3 cells (1000 cells/well) were added to the upper chamber

in 45 μ L serum-free medium, while in the lower chamber, as the chemoattractant, the serum-free CM of NHDF_{CI} or NHDF_{SK} was used; cells invading in response to the CM of untreated fibroblasts were used as controls.

The cells were allowed to invade the Matrigel[®] for 24 h at 37°C in a 5% CO₂ atmosphere. The non-invading cells on the upper surface of the membrane were removed with a cotton swab. Cells were fixed in 1% crystal violet in methanol. Invading cells in three adjacent microscope fields for each membrane were counted at x20 magnification.

Zymography assays

Serum-free CM of NHDF_{CI} or NHDF_{SK} was normalized by equal volume and equal cell number to perform both gelatin and casein-plasminogen zymography assays. Gelatin zymography was performed using 7.5% SDS-PAGE that was copolymerized with 1 mg/mL gelatin type B (Sigma-Aldrich; Merck KGaA); the CM was diluted in SDS-PAGE sample buffer under nonreducing conditions without heating. After electrophoresis, the gels were washed three times, for 15 minutes each, in 50 mM Tris-HCl (pH 7.4) containing 2.5% Triton X-100 (Sigma-Aldrich; Merck KGaA) under agitation at room temperature, and then incubated overnight in Tris buffer (50 mM Tris-HCl, pH 7.4, containing 5 mM CaCl₂ and 120 mM NaCl) at 37°C. The gels were then stained with Coomassie Blue R 250 (Bio-Rad Laboratories, Inc.) dissolved in a mixture of methanol:acetic acid:water (4:1:5) for 30 minutes, and were destained in the same solution without dye.

The PAs (plasminogen activators) in the CM were examined by casein-plasminogen zymography. The CM under non-reducing conditions and without heating, was separated by electrophoresis via 10% SDS-PAGE, which was copolymerized with 0.2% casein (Sigma-Aldrich; Merck KGaA) and 10 mg/mL human plasminogen (Sigma-Aldrich; Merck KGaA). After electrophoresis, the gel was washed three times for 30 minutes in Tris 50 mM pH 7.4 with 2.5% Triton X-100 and incubated for 48 h at 37°C in Tris-HCl 50 mM pH 7.4 + 0.02% Na₃N. The gels were stained and destained as described previously. The activity of gelatinases and PAs appeared as clear and distinct bands, which indicated proteolysis of the substrate, on a blue background. Digestion bands were quantified with Image J software (National Institutes of Health, Bethesda, MD, USA).

Migration assays

The migration of normal fibroblasts and of both ovarian cell lines was tested in response to the CM of EV-treated fibroblasts (set in the lower chambers, same volume for each sample). Cells migrating in response to the CM from untreated fibroblasts were used as controls.

Briefly, cells were detached, washed three times in serum-free DMEM, and seeded on the upper wells/chambers (5000 cells/well in 55 μ L serum-free DMEM medium) of the modified Boyden chambers. Gelatin-coated polycarbonate membranes with 8- μ m pores were used to separate the upper wells from the lower ones. Each condition to be tested was analyzed in triplicate. The chambers were incubated for 24 hours at 37°C in a CO₂ incubator, then migrated cells were fixed with pure

methanol and stained with 1% crystal violet in methanol. The number of cells migrating to the lower surface of the polycarbonate membrane was counted in five random x20 fields within each well under a microscope. The mean number of cells per field was calculated as the cell count.

Statistical analysis

Data are expressed as the mean and standard deviation (SD) or standard error of the mean (SEM). The use of either SD or SEM is specifically indicated in the figure legends. Errors were derived from at least 3 independent replicates. Comparisons between the means of control groups and treated groups were performed using 2-tailed Student's t-tests and the results were considered to be statistically significant when $p < 0.05$ (*), $p < 0.01$ (**), $p < 0.005$ (***) or $p < 0.001$ (****).

Disclosure of interest

The authors report no conflict of interest.

ORCID

Ilaria Giusti  <http://orcid.org/0000-0002-7982-471X>
 Marianna Di Francesco  <http://orcid.org/0000-0002-8418-135X>
 Sandra D'Ascenzo  <http://orcid.org/0000-0003-2820-2459>
 Maria Grazia Palmerini  <http://orcid.org/0000-0002-3985-0112>
 Guido Macchiarelli  <http://orcid.org/0000-0002-9182-0586>
 Gaspare Carta  <http://orcid.org/0000-0003-0424-6676>
 Vincenza Dolo  <http://orcid.org/0000-0003-0424-6676>

References

- Gould SJ, Raposo G. As we wait: coping with an imperfect nomenclature for extracellular vesicles. *J Extracell Vesicles*. 2013;2:20389. doi:10.3402/jev.v2i0.20389. PMID:24009890.
- Turturici G, Tinnirello R, Sconzo G, Geraci F. Extracellular membrane vesicles as a mechanism of cell-to-cell communication: advantages and disadvantages. *Am J Physiol Cell Physiol*. 2014;306(7):C621-33. doi:10.1152/ajpcell.00228.2013. PMID:24452373.
- Dolo V, D'Ascenzo S, Giusti I, Millimaggi D, Taraboletti G, Pavan A. Shedding of membrane vesicles by tumor and endothelial cells. *Ital J Anat Embryol*. 2005;110(2 suppl 1):127-33. PMID:16101030.
- Webber J, Yeung V, Clayton A. Extracellular vesicles as modulators of the cancer microenvironment. *Semin Cell Dev Biol*. 2015;40:27-34. doi:10.1016/j.semcdb.2015.01.013. PMID:25662446.
- Maas SL, Breakefield XO, Weaver AM. Extracellular Vesicles: Unique Intercellular Delivery Vehicles. *Trends Cell Biol*. 2017;27(3):172-88. doi:10.1016/j.tcb.2016.11.003. PMID:27979573.
- Giusti I, Dolo V. Extracellular vesicles in prostate cancer: new future clinical strategies? *Biomed Res Int*. 2014;2014:561571. doi:10.1155/2014/561571. PMID:24707491.
- Giusti I, D'Ascenzo S, Dolo V. Microvesicles as potential ovarian cancer biomarkers. *Biomed Res Int*. 2013;2013:703048. doi:10.1155/2013/703048. PMID:23484144.
- Giusti I, Di Francesco M, Dolo V. Extracellular Vesicles in Glioblastoma: Role in Biological Processes and in Therapeutic Applications. *Curr Cancer Drug Targets* 2017;17(3):221-35. doi:10.2174/1568009616666160813182959. PMID:27528364.
- Robbins PD, Morelli AE. Regulation of immune responses by extracellular vesicles. *Nat Rev Immunol*. 2014;14(3):195-208. doi:10.1038/nri3622. PMID:24566916.
- Owens AP 3, Mackman N. Microparticles in hemostasis and thrombosis. *Circ Res*. 2011;108(10):1284-97. doi:10.1161/CIRCRESAHA.110.233056. PMID:21566224.

11. Frühbeis C, Fröhlich D, Kuo WP, Krämer-Albers EM. Extracellular vesicles as mediators of neuron-glia communication. *Front Cell Neurosci* 2013;7:182. doi:10.3389/fncel.2013.00182. PMID:24194697.
12. De Jong OG, Van Balkom BW, Schiffelers RM, Bouten CV, Verhaar MC. Extracellular vesicles: potential roles in regenerative medicine. *Front Immunol.* 2014;5:608. doi:10.3389/fimmu.2014.00608. PMID:25520717.
13. Gaceb A, Martinez MC, Andriantsitohaina R. Extracellular vesicles, new players in cardiovascular diseases. *Int J Biochem Cell Biol.* 2014;50:24–28. doi:10.1016/j.biocel.2014.01.018. PMID:24509128.
14. Candelario KM, Steindler DA. The role of extracellular vesicles in the progression of neurodegenerative disease and cancer. *Trends Mol Med.* 2014;20(7):368–74. doi:10.1016/j.molmed.2014.04.003. PMID:24835084.
15. Millimaggi D, Mari M, D'Ascenzo S, Carosa E, Jannini EA, Zucker S, Carta G, Pavan A, Dolo V. Tumor vesicle-associated CD147 modulates the angiogenic capability of endothelial cells. *Neoplasia.* 2007;9(4):349–57. doi:10.1593/neo.07133. PMID:17460779.
16. Kosaka N, Iguchi H, Hagiwara K, Yoshioka Y, Takeshita F, Ochiya T. Neutral sphingomyelinase 2 (nSMase2)-dependent exosomal transfer of angiogenic microRNAs regulate cancer cell metastasis. *J Biol Chem.* 2013;288(15):10849–59. doi:10.1074/jbc.M112.446831. PMID:23439645.
17. Giusti I, D'Ascenzo S, Millimaggi D, Taraboletti G, Carta G, Franceschini N, Pavan A, Dolo V. Cathepsin B mediates the pH-dependent proinvasive activity of tumor-shed microvesicles. *Neoplasia.* 2008;10(5):481–8. doi:10.1593/neo.08178. PMID:18472965.
18. Lv MM, Zhu XY, Chen WX, Zhong SL, Hu Q, Ma TF, Zhang J, Chen L, Tang JH, Zhao JH. Exosomes mediate drug resistance transfer in MCF-7 breast cancer cells and a probable mechanism is delivery of P-glycoprotein. *Tumour Biol.* 2014;35(11):10773–9. doi:10.1007/s13277-014-2377-z. PMID:25077924.
19. Ge R, Tan E, Sharghi-Namini S, Asada HH. Exosomes in Cancer Microenvironment and Beyond: have we Overlooked these Extracellular Messengers? *Cancer Microenviron.* 2012;5(3):323–32. doi:10.1007/s12307-012-0110-2. PMID:22585423.
20. Luo Z, Wang Q, Lau WB, Lau B, Xu L, Zhao L, Yang H, Feng M, Xuan Y, Yang Y, et al. Tumor microenvironment: The culprit for ovarian cancer metastasis? *Cancer Lett.* 2016;377(2):174–82. doi:10.1016/j.canlet.2016.04.038. PMID:27131957.
21. Siegel RL, Miller KD, Jemal A. Cancer Statistics 2017. *CA Cancer J Clin.* 2017;67(1):7–30. doi:10.3322/caac.21387. PMID:28055103.
22. Yeung TL, Leung CS, Li F, Wong SS, Mok SC. Targeting Stromal-Cancer Cell Crosstalk Networks in Ovarian Cancer Treatment. *Biomolecules.* 2016;6(1):3. doi:10.3390/biom6010003. PMID:26751490.
23. Kalluri R. The biology and function of fibroblasts in cancer. *Nat Rev Cancer.* 2016;16(9):582–98. doi:10.1038/nrc.2016.73. PMID:27550820.
24. Erdogan B, Webb DJ. Cancer-associated fibroblasts modulate growth factor signaling and extracellular matrix remodeling to regulate tumor metastasis. *Biochem Soc Trans.* 2017;45(1):229–36. doi:10.1042/BST20160387. PMID:28202677.
25. Kuzet SE, Gaggioli C. Fibroblast activation in cancer: when seed fertilizes soil. *Cell Tissue Res.* 2016;365(3):607–19. doi:10.1007/s00441-016-2467-x. PMID:27474009.
26. Ostman A, Augsten M. Cancer-associated fibroblasts and tumor growth-bystanders turning into key players. *Curr Opin Genet Dev.* 2009;19(1):67–73. doi:10.1016/j.gde.2009.01.003. PMID:19211240.
27. Xing F, Saidou J, Watabe K. Cancer associated fibroblasts (CAFs) in tumor microenvironment. *Front Biosci (Landmark Ed).* 2010;15:166–79. doi:10.2741/3613. PMID:20036813.
28. Mishra P, Banerjee D, Ben-Baruch A. Chemokines at the crossroads of tumor-fibroblast interactions that promote malignancy. *J Leukoc Biol.* 2011;89(1):31–39. doi:10.1189/jlb.0310182. PMID:20628066.
29. Bruzzese F, Hägglöf C, Leone A, Sjöberg E, Roca MS, Kiflemariam S, Sjöblom T, Hammarsten P, Egevad L, Bergh A, et al. Local and systemic protumorigenic effects of cancer-associated fibroblast-derived GDF15. *Cancer Res.* 2014;74(13):3408–17. doi:10.1158/0008-5472.CAN-13-2259. PMID:24780757.
30. Subramaniam KS, Tham ST, Mohamed Z, Woo YL, Adenan NAM, Chung I. Cancer-Associated Fibroblasts Promote Proliferation of Endometrial Cancer Cells. *PLoS One.* 2013;8(7):e68923. doi:10.1371/journal.pone.0068923. PMID:23922669.
31. Webber J, Steadman R, Mason MD, Tabi Z, Clayton A. Cancer exosomes trigger fibroblast to myofibroblast differentiation. *Cancer Res.* 2010;70(23):9621–30. doi:10.1158/0008-5472.CAN-10-1722. PMID:21098712.
32. Cho JA, Park H, Lim EH, Lee KW. Exosomes from breast cancer cells can convert adipose tissue-derived mesenchymal stem cells into myofibroblast-like cells. *Int J Oncol.* 2012;40(1):130–8. doi:10.3892/ijo.2011.1193. PMID:21904773.
33. Castellana D, Zobairi F, Martinez MC, Panaro MA, Mitolo V, Freyssi-net JM, Kunzelmann C. Membrane microvesicles as actors in the establishment of a favorable prostatic tumoral niche: a role for activated fibroblasts and CX3CL1-CX3CR1 axis. *Cancer Res.* 2009;69(3):785–93. doi:10.1158/0008-5472.CAN-08-1946. PMID:19155311.
34. Cho JA, Park H, Lim EH, Kim KH, Choi JS, Lee JH, Shin JW, Lee KW. Exosomes from ovarian cancer cells induce adipose tissue-derived mesenchymal stem cells to acquire the physical and functional characteristics of tumor-supporting myofibroblasts. *Gynecol Oncol.* 2011;123(2):379–86. doi:10.1016/j.ygyno.2011.08.005.
35. Paggetti J, Haderk F, Seiffert M, Janji B, Distler U, Ammerlaan W, Kim YJ, Adam J, Lichter P, Solary E, et al. Exosomes released by chronic lymphocytic leukemia cells induce the transition of stromal cells into cancer-associated fibroblasts. *Blood.* 2015;126(9):1106–17. doi:10.1182/blood-2014-12-618025. PMID:26100252.
36. Gu J, Qian H, Shen L, Zhang X, Zhu W, Huang L, Yan Y, Mao F, Zhao C, Shi Y, et al. Gastric cancer exosomes trigger differentiation of umbilical cord derived mesenchymal stem cells to carcinoma-associated fibroblasts through TGF- β /Smad pathway. *PLoS One.* 2010;7(12):e24465. doi:10.1371/journal.pone.0052465.
37. Mitra AK, Zillhardt M, Hua Y, Tiwari P, Murmann AE, Peter ME, Lengyel E. MicroRNAs reprogram normal fibroblasts into cancer-associated fibroblasts in ovarian cancer. *Cancer Discov.* 2012;2(12):1100–8. doi:10.1158/2159-8290.CD-12-0206. PMID:23171795.
38. Shiga K, Hara M, Nagasaki T, Sato T, Takahashi H, Takeyama H. Cancer-Associated Fibroblasts: Their Characteristics and Their Roles in Tumor Growth. *Cancers (Basel).* 2015;7(4):2443–58. doi:10.3390/cancers7040902. PMID:26690480.
39. Mezawa Y, Orimo A. The roles of tumor- and metastasis-promoting carcinoma-associated fibroblasts in human carcinomas. *Cell Tissue Res.* 2016;365(3):675–89. doi:10.1007/s00441-016-2471-1. PMID:27506216.
40. Ishii G, Ochiai A, Neri S. Phenotypic and functional heterogeneity of cancer-associated fibroblast within the tumor microenvironment. *Adv Drug Deliv Rev.* 2016;99(Pt B):186–96. doi:10.1016/j.addr.2015.07.007. PMID:26278673.
41. Millimaggi D, Mari M, D'Ascenzo S, Giusti I, Pavan A, Dolo V. Vasculogenic mimicry of human ovarian cancer cells: role of CD147. *Int J Oncol.* 2009;35:1423–8. PMID:19885565.
42. Merlino G, Miodini P, Paolini B, Carcangiu ML, Gennaro M, Dugo M, Daidone MG, Cappelletti V. Stromal Activation by Tumor Cells: An in Vitro Study in Breast Cancer. *Microarrays (Basel).* 2016;5(2):pii: E10. doi:10.3390/microarrays5020010.
43. Kayamori K, Katsube K, Sakamoto K, Ohyama Y, Hirai H, Yukimori A, Ohata Y, Akashi T, Saitoh M, Harada K, et al. NOTCH3 Is Induced in Cancer-Associated Fibroblasts and Promotes Angiogenesis in Oral Squamous Cell Carcinoma. *PLoS One.* 2016;11(4):e0154112. doi:10.1371/journal.pone.0154112. PMID:27124156.
44. Momen-Heravi F. Isolation of Extracellular Vesicles by Ultracentrifugation. *Methods Mol Biol.* 2017;1660:25–32. doi:10.1007/978-1-4939-7253-1_3. PMID:28828645.
45. Shimoda M, Principe S, Jackson HW, Luga V, Fang H, Molyneux SD, Shao YW, Aiken A, Waterhouse PD, Karamboulas C, et al. Loss of the Timp gene family is sufficient for the acquisition of the CAF-like cell state. *Nat Cell Biol.* 2014;16(9):889–901. doi:10.1038/ncb3021. PMID:25150980.
46. Wolf K, Wu YI, Liu Y, Geiger J, Tam E, Overall C, Stack MS, Friedl P. Multi-step pericellular proteolysis controls the transition from individual to collective cancer cell invasion. *Nat Cell Biol.* 2007;9(8):893–904. doi:10.1038/ncb1616. PMID:17618273.
47. Santi A, Caselli A, Ranaldi F, Paoli P, Mugnaioni C, Michelucci E, Cirri P. Cancer associated fibroblasts transfer lipids and proteins to

- cancer cells through cargo vesicles supporting tumor growth. *Biochim Biophys Acta*. 2015;1853(12):3211–23. doi:10.1016/j.bbamcr.2015.09.013. PMID:26384873.
48. Luga V, Zhang L, Vitoria-Petit AM, Ogunjimi AA, Inanlou MR, Chiu E, Buchanan M, Hosein AN, Basik M, Wrana JL. Exosomes mediate stromal mobilization of autocrine Wnt-PCP signaling in breast cancer cell migration. *Cell*. 2012;151(7):1542–56. doi:10.1016/j.cell.2012.11.024. PMID:23260141.
49. Hu Y, Yan C, Mu L, Huang K, Li X, Tao D, Wu Y, Qin J. Fibroblast-Derived Exosomes Contribute to Chemoresistance through Priming Cancer Stem Cells in Colorectal Cancer. *PLoS One* 2015;10(5):e0125625. doi:10.1371/journal.pone.0125625. PMID:25938772.
50. Nakamura T, Matsumoto K, Kiritoshi A, Tano Y, Nakamura T. Induction of hepatocyte growth factor in fibroblasts by tumor-derived factors affects invasive growth of tumor cells: in vitro analysis of tumor-stromal interactions. *Cancer Res*. 1997;57(15):3305–13. PMID:9242465.
51. Murata T, Mizushima H, Chinen I, Moribe H, Yagi S, Hoffman RM, Kimura T, Yoshino K, Ueda Y, Enomoto T, et al. HB-EGF and PDGF mediate reciprocal interactions of carcinoma cells with cancer-associated fibroblasts to support progression of uterine cervical cancers. *Cancer Res*. 2011;71(21):6633–42. doi:10.1158/0008-5472.CAN-11-0034. PMID:22009535.
52. Teng F, Tian WY, Wang YM, Zhang YF, Guo F, Zhao J, Gao C, Xue FX. Cancer-associated fibroblasts promote the progression of endometrial cancer via the SDF-1/CXCR4 axis. *J Hematol Oncol*. 2016;9:8. doi:10.1186/s13045-015-0231-4. PMID:26851944.
53. Bai YP, Shang K, Chen H, Ding F, Wang Z, Liang C, Xu Y, Sun MH, Li YY. FGF-1/-3/FGFR4 signaling in cancer-associated fibroblasts promotes tumor progression in colon cancer through Erk and MMP-7. *Cancer Sci*. 2015;106(10):1278–87. doi:10.1111/cas.12745. PMID:26183471.
54. Dolo V, Ginestra A, Violini S, Miotti S, Festuccia C, Miceli D, Migliavacca M, Rinaudo C, Romano FM, Brisdelli F, et al. Ultrastructural and phenotypic characterization of CABA I a new human ovarian cancer cell line. *Oncol Res*. 1997;9(3):129–38. PMID:9220498.